

## **A benzoic acid terpyridine-based cyclometalated iridium (III) complex as two-photon fluorescence probe for imaging nuclear histidine**

Qiong Zhang<sup>¶a</sup>, Xin Lu<sup>¶a</sup>, Hui Wang<sup>¶a,c</sup>, Xiaohe Tian<sup>b\*</sup>, Aidong Wang<sup>d</sup>, Hongping Zhou<sup>a</sup>, Jieying Wu<sup>a</sup> and Yupeng Tian<sup>a,e\*</sup>

[a] Department of Chemistry, Key Laboratory of Functional Inorganic Material Chemistry of Anhui Province, Anhui University, Hefei 230601, P. R. China

[b] School of Life Science, Anhui University, Hefei 230601, P.R. China

[c] Department of Chemistry, Wannan Medical College, Wuhu 241002, P. R. China

[d] School of Chemistry and Chemical Engineering, Huangshan University, Huangshan, P. R. China.

[e] State Key Laboratory of Coordination Chemistry, Nanjing University, Nanjing 210093, P. R. China

<sup>¶</sup>These authors contributed equally to this work.

*E-mail address:* [xiaohe.t@ahu.edu.cn](mailto:xiaohe.t@ahu.edu.cn); [yptian@ahu.edu.cn](mailto:yptian@ahu.edu.cn)

Materials and instruments .....	3
Optical Measurements.....	3
Synthesis of Ir1 .....	3
Synthesis of Ir2 .....	4
Synthesis of Ir3 .....	5
Computational details .....	5
Molecular docking Method.....	5
Two-Photon Excited Fluorescence (TPEF) Spectroscopy and Two-Photon Absorption (2PA) Cross-Section .....	5
Biological experiments details .....	6
Cytotoxicity assays in cells .....	6
Cell Imaging.....	7
Interaction of Ir1 with amino acids and biomolecules .....	7
Formation of HepG2 MCSs.....	8
Confocal cell imaging .....	8
Cellular uptake and distribution (ICP-MS).....	9

TEM cell imaging .....	9
Scheme S1 The synthetic route for complexes Ir1-Ir3.....	10
Fig S1 The <sup>1</sup> H-NMR spectrum of Ir1.....	10
Fig S2 The <sup>13</sup> C-NMR spectrum of Ir1. ....	11
Fig S3 The MALDI-TOF-MS spectra of Ir1~Ir3.....	12
Fig S5 Linear absorption and linear emission spectra of Ir1 .....	13
Fig. S7 OPEF spectra of Ir1([Ir1]=10 μM) obtained in different NaOH concentrations.....	14
Fig. S8. Luminescence emission spectra of Ir1 upon addition of histidine .....	14
Fig S10 Changes in the luminescence emission spectra of Ir1 with various amounts of BSA.....	15
Fig. S11 Changes in the luminescence emission spectra of Ir1 with various amounts of 6×His ...	15
Fig. S12 Two-photon fluorescence spectra of Ir1 in the presence or absence of His .....	15
Fig. S13 (a) <sup>1</sup> H NMR spectra change and of Ir1 in the absence and presence of 10 histidine. ....	16
Fig S14 Cytotoxicity data results of Ir1 obtained from the MTT assay.....	16
Fig S15 The photobleaching property of Ir1 .....	17
Fig S16 Subcellular distribution of iridium in HepG2 cell incubation with Ir1. ....	17
Fig S17 Confocal two-photon fluorescence images.....	17
Fig S18 Two-photon micrographs for living HELF cells treated with Ir1 .....	18
Fig S19 Mechanism of cellular uptake of Ir1 (scale bar = 20μm) .....	18
Fig S20 Two-photon fluorescence images of the 3D multicellular spheroids of HepG2 cells .....	19
Table S1 The photophysical data of the complex Ir1 and Ir1-His in different solvents .....	19
Table S2 Calculated triplet transitions and the frontier orbitals of Ir1 .....	19
Table S3 Calculated triplet transitions and the frontier orbitals of Ir1-histidine. ....	19

## Materials and instruments

Chemicals and reagents were purchased from commercial sources and used without further purification unless otherwise stated. MALDI-TOF mass spectra were recorded using Bruker Autoflex III Smartbeam.  $^1\text{H}$  NMR,  $^{13}\text{C}$  NMR and  $^{119}\text{Sn}$  NMR were recorded on a Bruker 400 Ultrashield spectrometer using  $\text{d}_6\text{-DMSO}$  as solvent at room temperature and TMS as the internal standard. IR spectra ( $4000\text{-}400\text{ cm}^{-1}$ ) were recorded on a Nicolet FT-IR 870 SX spectrophotometer with KBr pellets.

UV-vis absorption spectra were recorded on a SHIMADZU UV-3600 spectrophotometer. Emission spectra were recorded on a HITACHI F-2500 spectrofluorophotometer at room temperature. For time-resolved fluorescence measurements, the fluorescence signals were collimated and focused onto the entrance slit of a monochromator with the output plane equipped with a photomultiplier tube (HORIBA HuoroMax-4P). The decays were analyzed by ‘least-squares’. The quality of the exponential fits was evaluated by the goodness of fit ( $\chi^2$ ).

## Optical Measurements

The OPA spectra were measured on a UV-3600 spectrophotometer. The OPEF measurements were performed by using an F-2500 fluorescence spectrophotometer. The concentration of sample solution was  $1.0 \times 10^{-5}$  mol/L. The fluorescence quantum yields ( $\Phi$ ) were determined by using coumarin 307 as the reference according to the literature method [1]. Quantum yields were corrected as follows:

$$\Phi_s = \Phi_r \left( \frac{A_r(\lambda_r)}{A_s(\lambda_s)} \right) \left( \frac{n_s^2}{n_r^2} \right) \frac{\int F_s}{\int F_r}$$

Where the  $s$  and  $r$  indices designate the sample and reference samples, respectively,  $A$  is the absorbance at  $\lambda_{\text{exc}}$ ,  $n$  is the average refractive index of the appropriate solution, and  $D$  is the

integrated area under the corrected emission spectrum [2]. For time-resolved fluorescence measurements, the fluorescence signals were collimated and focused onto the entrance slit of a monochromator with the output plane equipped with a photomultiplier tube (HORIBA HuoroMax-4P). The decays were analyzed by 'least-squares'. The quality of the exponential fits was evaluated by the goodness of fit ( $\chi^2$ ).

### Synthesis of Ir1

A mixture of the bridged-dimer  $[\text{Ir}(\text{C}^{\wedge}\text{N})_2(\mu\text{-Cl})_2]_2$  (0.19 mmol, 0.199 g) and **L** [3] (0.38 mmol, 0.13 g), taken in 100 mL of methanol- dichloromethane (2:1, v/v) degassed solvent system, was heated under reflux in an inert atmosphere of  $\text{N}_2$  in the dark for 24 h. The reaction mixture was then brought to room temperature, and 10-excess of saturated  $\text{KPF}_6$  in degassed methanol was added to it with an additional stirring for 2 h. The solvent was then evaporated under vacuum. The orange solid was dissolved in  $\text{CH}_2\text{Cl}_2$  and purified by column chromatography on silica gel eluted with  $\text{CH}_2\text{Cl}_2$ /methanol (10:1, v/v). Yield: 53 %. Anal. Calcd. for  $\text{C}_{33}\text{H}_{23}\text{N}_4\text{IrPF}_6$ : C, 46.92; H, 2.74; N, 6.63. Found: C, 46.86; H, 2.74; N, 6.61. IR (KBr,  $\text{cm}^{-1}$ ): 3430, 3045, 1698, 1608, 1582, 1478, 1438, 1423, 1395, 1316, 1270, 1235, 1163, 1064, 1009, 841, 775, 756, 734, 700, 557.  $^1\text{H-NMR}$  (400 MHz,  $\text{d}_6\text{-DMSO}$ ,  $\delta/\text{ppm}$ ): 5.78 (d, 2H), 6.265 (t, 1H), 6.558 (t, 1H), 6.745 (t, 1H), 6.817 (d, 1H), 6.922 (t, 1H), 6.988 (m, 1H), 7.096 (t, 1H), 7.224 (t, 1H), 7.308 (t, 1H), 7.491 (d, 1H), 7.553 (d, 1H), 7.667 (m, 2H), 7.826 (d, 1H), 7.907 (t, 1H), 7.974 (m, 2H), 8.120 (m, 4H), 8.224 (d, 1H), 8.335 (m, 3H), 8.853 (m, 1H), 9.223 (d, 2H), 13.056 (s, 1H).  $^{13}\text{C-NMR}$  (100 MHz,  $\text{d}_6\text{-DMSO}$ ,  $\delta/\text{ppm}$ ): 119.58, 120.06, 122.95, 123.21, 123.84, 124.95, 125.97, 128.10, 129.09, 129.95, 131.59, 132.66, 135.87, 135.90, 138.52, 139.45, 142.46, 143.11, 147.10, 148.15, 148.89, 149.11, 151.87, 155.55, 156.45, 157.55, 162.76, 165.81, 166.73, 167.49. MS (MALDI-TOF) [ $m/z\text{-PF}_6$ ]: 854.653. Calculated: 999.17.

### Synthesis of Ir2

Complex **Ir2** was synthesized in a similar manner to **Ir1** with using bipyridine 0.09 g (0.38 mmol). A bright yellow solid was obtained. Yield: 65 %. Anal. Calcd. for  $\text{C}_{26}\text{H}_{19}\text{N}_4\text{IrPF}_6$ : C, 43.09; H, 2.64; N, 7.73. Found: C, 43.13; H, 2.64; N, 7.71. IR (KBr,  $\text{cm}^{-1}$ ): 3047, 1606, 1582, 1565,

1479, 1450, 1429, 1227, 1165, 1029, 841, 773, 757, 733, 557.  $^1\text{H}$  NMR (400 MHz,  $\text{d}_6\text{-DMSO}$ ,  $\delta/\text{ppm}$ ) 8.87 (t,  $J = 7.4$  Hz, 5H), 8.34 – 8.25 (m, 5H), 8.24 – 8.05 (m, 7H), 7.95 (s, 2H), 7.89 (s, 2H), 7.79 (d,  $J = 7.8$  Hz, 2H), 7.60 (dd,  $J = 15.8, 7.3$  Hz, 7H), 7.48 (dd,  $J = 21.3, 6.8$  Hz, 5H), 7.29 (s, 2H), 7.18 (s, 2H), 7.08 (s, 2H), 6.90 (s, 2H), 6.72 (s, 3H), 6.53 (s, 2H), 6.23 (s, 2H), 5.80 – 5.72 (m, 3H), 5.33 (d,  $J = 7.5$  Hz, 2H), 3.31 (s, 30H), 2.49 (d,  $J = 1.4$  Hz, 33H), 1.98 (s, 1H), -0.01 (s, 1H).  $^{13}\text{C}$  NMR (101 MHz,  $\text{d}_6\text{-DMSO}$ ,  $\delta/\text{ppm}$ ) 40.12 (s, 1H), 39.91 (s, 5H), 39.71 (s, 8H), 39.50 (s, 8H), 39.29 (s, 7H), 39.08 (s, 4H), 38.87 (s, 1H). MS (MALDI-TOF) [ $m/z\text{-PF}_6$ ]: 734.5. Calculated: 879.15.

### Synthesis of Ir3

Complex **Ir3** was synthesized in a similar manner to **Ir1** with using bipyridine 0.06 g (0.38 mmol). A bright orange solid was obtained. Yield: 68 %. Anal. Calcd. for  $\text{C}_{21}\text{H}_{16}\text{N}_3\text{IrPF}_6$ : C, 38.95; H, 2.49; N, 17.60. Found: C, 39.01; H, 2.48; N, 17.57. IR(KBr,  $\text{cm}^{-1}$ ): 3433, 1607, 1582, 1479, 1443, 1422, 1162, 1301, 878, 840, 758, 732, 557.  $^1\text{H}$  NMR (400 MHz,  $\text{d}_6\text{-DMSO}$ ,  $\delta/\text{ppm}$ ) 8.87 (d,  $J = 8.2$  Hz, 5H), 8.87 (d,  $J = 8.2$  Hz, 5H), 8.27 (t,  $J = 7.0$  Hz, 10H), 8.27 (t,  $J = 7.0$  Hz, 10H), 7.99 – 7.89 (m, 10H), 7.99 – 7.82 (m, 15H), 7.86 (d,  $J = 5.3$  Hz, 5H), 7.74 – 7.65 (m, 5H), 7.73 – 7.65 (m, 5H), 7.61 (d,  $J = 5.6$  Hz, 5H), 7.61 (d,  $J = 5.6$  Hz, 5H), 7.15 (t,  $J = 6.6$  Hz, 5H), 7.15 (t,  $J = 6.6$  Hz, 5H), 7.01 (t,  $J = 7.5$  Hz, 5H), 7.01 (t,  $J = 7.5$  Hz, 5H), 6.90 (t,  $J = 7.4$  Hz, 5H), 6.90 (t,  $J = 7.4$  Hz, 5H), 6.18 (d,  $J = 7.5$  Hz, 5H), 6.18 (d,  $J = 7.5$  Hz, 5H), 5.75 (s, 1H), 5.75 (s, 1H), 3.34 (s, 44H), 2.49 (s, 55H), 1.22 (s, 2H), -0.01 (s, 2H).  $^{13}\text{C}$  NMR (101 MHz,  $\text{d}_6\text{-DMSO}$ ,  $\delta/\text{ppm}$ ) 40.12 (s, 1H), 39.91 (s, 4H), 39.70 (s, 3H), 39.50 (s, 8H), 39.29 (s, 5H), 39.08 (s, 3H), 38.87 (s, 1H). MS (MALDI-TOF) [ $m/z\text{-PF}_6$ ]: 657.42. Calculated: 802.13.

### Computational details

Optimizations were carried out with B3LYP [LANL2DZ] without any symmetry restraints, and the TD-DFT {B3LYP[LANL2DZ]} calculations were performed on the optimized structure. All calculations, including optimizations and TD-DFT, were performed with the G09 software. Geometry optimization of the singlet ground state and the TD-DFT calculation of the lowest 25

singlet-singlet excitation energies were calculated with a basis set composed of 6-31G\* for C H N O P F atoms and the Lanl2dz basis set for Ir and Sn atoms were download from the EMSL basis set library.

### **Molecular docking Method**

Uses LigandFit Monte-Carlo techniques to generate ligand conformations and docks them into the active site using a shape-based initial docking [4]. The docked poses may optionally be minimized with CHARMM and evaluated with a set of scoring functions.

The following steps are performed:

1. Performs ligand docking using LigandFit
2. Minimizes docked poses using CHARMM
3. Scores poses

### **Two-Photon Excited Fluorescence (TPEF) Spectroscopy and Two-Photon Absorption (2PA) Cross-Section**

2PA cross-sections ( $\sigma$ ) of the samples were obtained by the two-photon excited fluorescence (TPEF) method with a femtosecond laser pulse and a Ti:sapphire system (690–1080 nm, 80 MHz, 140 fs) as the light source (Coherent, Inc., Chameleon Ultra II, area light source: 0.9503 mm<sup>2</sup>). The concentration of sample solution was 1.0×10<sup>-4</sup> M. Thus, the  $\delta$  values of samples were determined by the following Equation (1).  $\delta_s = \delta_r \cdot F_s \cdot \Phi_r \cdot C_r \cdot n_r / F_r \cdot \Phi_s \cdot C_s \cdot n_s$  where the subscripts “s” and “r” represent sample and reference (here, fluorescein in ethanol solution at a concentration of 1.0×10<sup>-4</sup> mol/L was used as reference), respectively. F is the overall fluorescence collection efficiency intensity of the fluorescence signal collected by the fiber spectra meter.  $\Phi$ ,  $n$  and  $c$  are the quantum yield of the fluorescence, the refractive index of solvent, and the concentration of the solution, respectively.

### **Biological experiments details**

Cells (including cancer cell and normal cell) were cultured in 25cm<sup>2</sup> culture flasks in DMEM,

supplemented with fetal bovine serum (10 %), penicillin (100 units/mL) and streptomycin (50 units/mL) at 37 °C in a CO<sub>2</sub> incubator (95 % relative humidity, 5 % CO<sub>2</sub>). Cells were seeded in 35 mm glass bottom cell culture dishes, at a density of  $1 \times 10^5$  cells and were allowed to grow when the cells reached more than 60 % confluence. The compounds were dissolved in DMSO with concentration of 1mM as stock solution, and the commercial dyes were prepared as 1mM PBS solution and diluted to working concentration as protocol required.

### **Cytotoxicity assays in cells**

To determine the cytotoxic effect of Ir complexes which treated over 24h as a period, the 5-dimethylthiazol-2-yl-2,5-diphenyltetrazolium bromide (MTT) assay was performed. When HepG2 cells reached ~70 % confluence, HepG2 cells were harvested by trypsin and plated in flat-bottom 96-well plates for 24 h. Prior to the treatment of Ir complexes, the medium was removed and replaced with fresh medium/DMSO = 99/1 (containing concentration of Ir complexes 1, 5, 10, 15  $\mu$ M). Subsequently, the treated cells were incubated for 24 h at 37 °C with 5% CO<sub>2</sub>. After that, the cells were treated with 5 mg/mL MTT (40  $\mu$ L/well) and incubated for another 4 h (37 °C, 5% CO<sub>2</sub>). Then medium was removed, the formazan crystals were dissolved in DMSO(150  $\mu$ L/well), and the absorbance at 490 nm was recorded. The cell viability (%) was calculated according to the following equation: cell viability % =  $OD_{490}(\text{sample})/OD_{490}(\text{control}) \times 100$ , where  $OD_{490}(\text{sample})$  represented the optical density of the wells treated with various concentrations of the compounds and  $OD_{490}(\text{control})$  represented that of the wells treated with DMEM + 10% FCS. Each concentration of Ir complexes covered eight wells which considered as one experimental group. And the averages and standard deviations were also reported. The reported percent of cell survival values are related to untreated control cells.

### **Cell Imaging**

HepG2, A549, Hela and HELF cells were seeded in 24-well glass bottom plates at a density of  $1 \times 10^4$  cells per well and grown for 96 hours. The cells were plated in 24 well glass-bottom plates (cellvis) and cultured for 48 h. The cells were solely incubated with 1 mL media/DMSO (v/v=99:1) containing various concentrations of compounds for 30 min (37 °C, 5% CO<sub>2</sub>). The excess

complexes were washed away by PBS for 3 times, after that the confocal microscopy imaging was carried out. For co-localization, the HepG2 cells were incubated with Nuclear Red<sup>®</sup> for 10 min after washed way the excess tracker by PBS for 3 times.

### **Interaction of Ir1 with amino acids and biomolecules**

The interaction of **Ir1** with amino acids, lysozyme, bovine serum albumin (BSA), polypeptides, ct-DNA and RNA has been investigated by luminescent emission titration. Herein, L-asparagine (Asp), L-arginine (Arg), L-ptoline (Pro), L-glycine (Gly), L-serine (Ser), L-glutamine (Gln), L-phenylalanine (Phe), L-valine (Val), L-isoleucine (Ile), L-leucine (Leu), L-lysine (Lys), L-threonine (Thr), L-methionine (Met), L-cysteine (Cys), L-glutamic acid (Glu), L-alanine (Ala), L-tryptophan (Try), L-tyrosine (Tyr), L-homocysteine (Hcy), and L-histidine (His) were used as examples of amino acids. In particular, the emission responses of **Ir1** to different amount of histidine were studied in detail.

The addition of peptides and proteins with different numbers of histidine residues induced an enhancement in the luminescence intensity of **Ir1** (Fig. S8). The time plot of the emission intensity of Ir1 interacting with (10 equiv.) histidine is displayed in Fig. S9. The maximal phosphorescence signal of Ir1 responding to histidine was reached within 10 min. In addition, the luminescence response of Ir1 to proteins with a relatively high abundance of histidine residues, such as BSA, and 6 histidine, was also investigated (Fig. S10 and S11)

### **Fixed cell and inhibitors studies**

HepG2 cell was cultured in glass-bottom dish for 48 h, after that the cell was washed by PBS for 3 times and then incubated with 4% paraformaldehyde (1 mL). After that, the fixed cell was washed with PBS for 3 times and 5 L Ir complexes ( $1 \times 10^{-3}$  M in DMSO) was added to the plate and cultured for another 30 min (37 °C, 5% CO<sub>2</sub>). For inhibitors study, cells incubated with 1 M of inhibitors (including 2-deoxy-D-glucose, NH<sub>4</sub>Cl, chloroquine, nocodazole, chlorpromazine, and colchicine, which dissolved in 1 mL culture medium without serum) for 30 min (37 °C, 5% CO<sub>2</sub>), then 5 μL Ir complexes ( $1 \times 10^{-3}$  M in DMSO) was added to the plate and cultured for

another 30 min (37 °C, 5% CO<sub>2</sub>). The imaging was carried out after the cells were washed by PBS for 3 times.

### **Formation of HepG2 MCSs**

In order to produce MCSs, a layer of poly(2-hydroxyethyl methacrylate) (polyHEMA) thin film was coated on the bottom of tissue culture flasks. To ensure sterile, polyHEMA coated flask must be exposed to ultraviolet light for 4 h before use. HepG2 monolayer cells incubated as mentioned above were trypsinized to give a single-cell suspension and count the cell numbers using a hemocytometer.  $5 \times 10^5$  cells in 5 mL of fresh DMEM medium was placed in a cell culture flask coated by polyHEMA. Cells were incubated at 37 °C in humidified atmosphere with 5 % CO<sub>2</sub> and the culture medium was replaced every other day. HepG2 MCSs (around 200 µm in diameter) formed spontaneously in 7 days.

3D MCSs pretreated with 10 µM **Ir1** respectively, for 5 h at 37 °C were carefully washed three times with PBS and subjected to confocal microscopy. The two-photon fluorescence images of sections along the z-axis were captured and stacked in the z-stack mode to give a final two-photon z-axis stack imaging.

### **Confocal cell imaging**

Confocal microscopy imaging was acquired with a Carl Zeiss LSM 710 confocal microscopy and 63X/100X oil-immersion objective lens. The incubated cells were excited at 405 nm for Ir1 for one-photon imaging, 633 nm for Nuclear Red<sup>®</sup>, and the emission signals were collected at  $580 \pm 20$  nm for Ir1,  $644 \pm 20$  nm for Nuclear Red<sup>®</sup>. Two-photon confocal microscopy imaging of Ir complexes was excited at 800 nm and the emission signals were detected in the region of 580-620 nm. Quantization by line plots was accomplished by using the software package provided by Carl Zeiss instrument.

### **Cellular uptake and distribution (ICP-MS)**

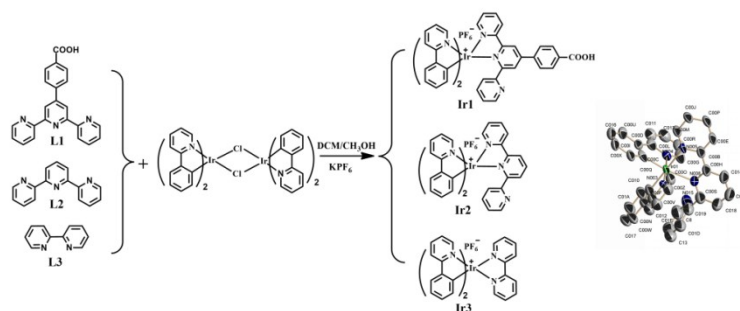
To quantify the levels of iridium in different subcellular compartments, ICP-MS was employed. Exponentially growing HepG2 cells were cultured in 25 cm<sup>2</sup> culture plates treated with the

iridium(III) complexes at a concentration of 10  $\mu\text{M}$  for 1 h. After digestion, HepG2 cells were counted and divided into two equal parts for the extraction of the nuclei and cytoplasm by using a nucleus extraction kit, respectively. **Ir1** was digested by 60%  $\text{HNO}_3$  at room temperature for 24 h. Each sample was diluted with Milli-Q water to achieve a final volume of 10 mL containing 3%  $\text{HNO}_3$ . The concentration of iridium in the three domains was determined by using an inductively coupled plasma mass spectrometer (Thermo Fisher Co., Ltd.).

### **TEM cell imaging**

For TEM, HepG2 cells were incubated with **Ir1** then fixed by using 3% glutaraldehyde and dehydrated with ethanol. For control cells and UV irradiation cells, secondary fixation was carried out in 1 % aqueous osmium tetroxide for 1 hour at room temperature, in order to visualize the membrane structures. For solely Iridium complex incubation group, the second fixation steps were ignored. The detailed protocols were listed as follow: For transmission electron microscopy, Cell specimens were received pelleted in Eppendorf tubes. Fresh 3 % glutaraldehyde in 0.1 M phosphate buffer was added to re-suspend the pellet to ensure optimal fixation, and left overnight at 4 °C. The specimens were then washed in 0.1 M-phosphate buffer at 4 °C, twice at 30 min intervals. Secondary fixation was carried out in 2 % aqueous osmium tetroxide for 2 hours at room temperature, followed by washing in buffer as above. Continuing at room temperature, this was followed by dehydration through a graded series of ethanol: 75% (15 min), 95% (15 min), 100% (15 min) and 100% (15 min). 100% ethanol was prepared by drying over anhydrous copper sulphate for 15min. The specimens were then placed in an intermediate solvent, propylene oxide, for two changes of 15mins duration. Resin infiltration was accomplished by placing the specimens in a 50/50 mixture of propylene oxide/Araldite resin. The specimens were left in this mixture overnight at room temperature. The specimens were left in full strength Araldite resin for 6-8 hrs at room temperature (with change of resin after 3-4 hrs) after which they were embedded in fresh Araldite resin for 48-72 hrs at 60 °C. Semi-thin sections approximately 0.5  $\mu\text{m}$  thick were cut on a Leica 10 ultramicrotome and stained with 1% Toluidine blue in Borax. Ultra-thin sections, approx. 70-90nm thick, were cut on a Leica ultramicrotome and stained for 25mins with saturated aqueous uranyl acetate followed by staining with Reynold's lead citrate for 5mins. The sections were

examined using a FEI Tecnai Transmission Electron Microscope at an accelerating voltage of 80kVv. Electron micrographs were taken using a Gatan digital camera.



Scheme S1 The synthetic route for complexes **Ir1-Ir3**.

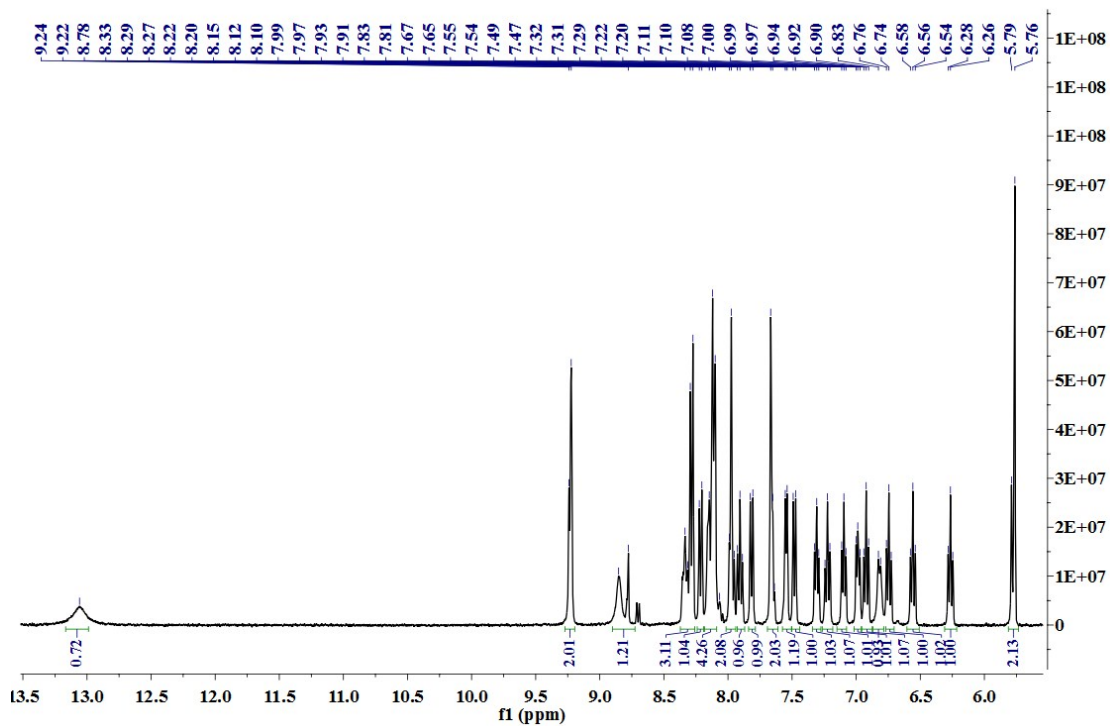


Fig S1 The  $^1\text{H-NMR}$  spectrum of **Ir1**.

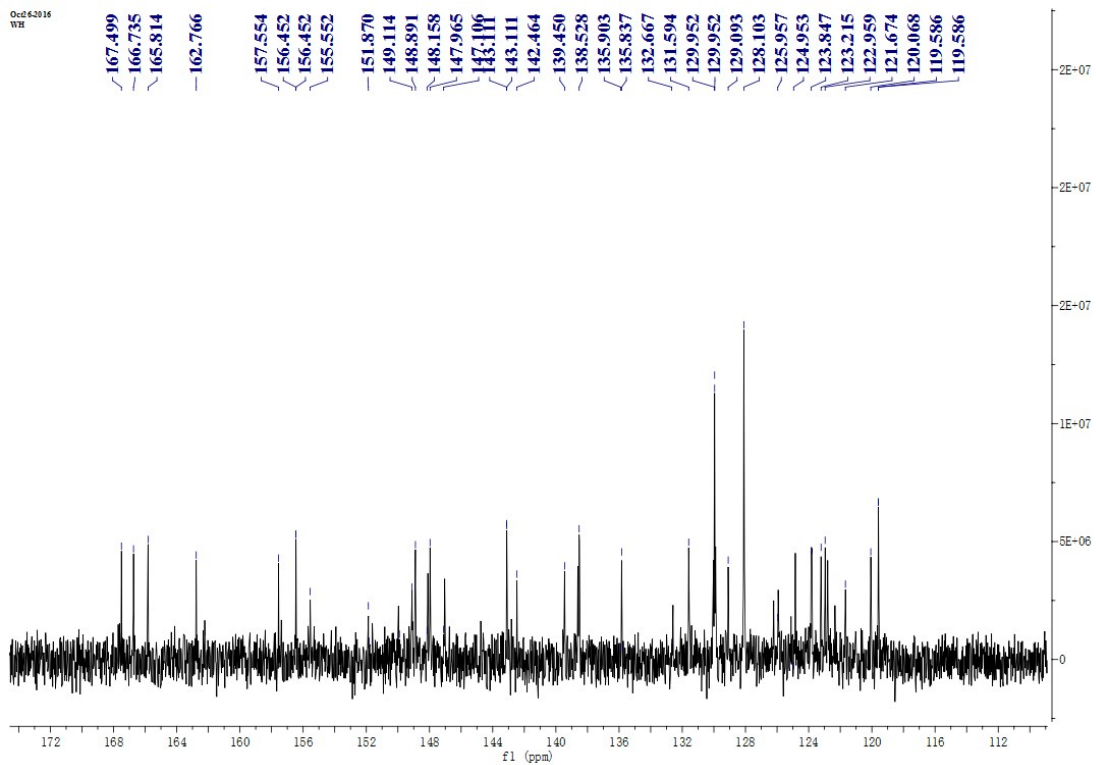
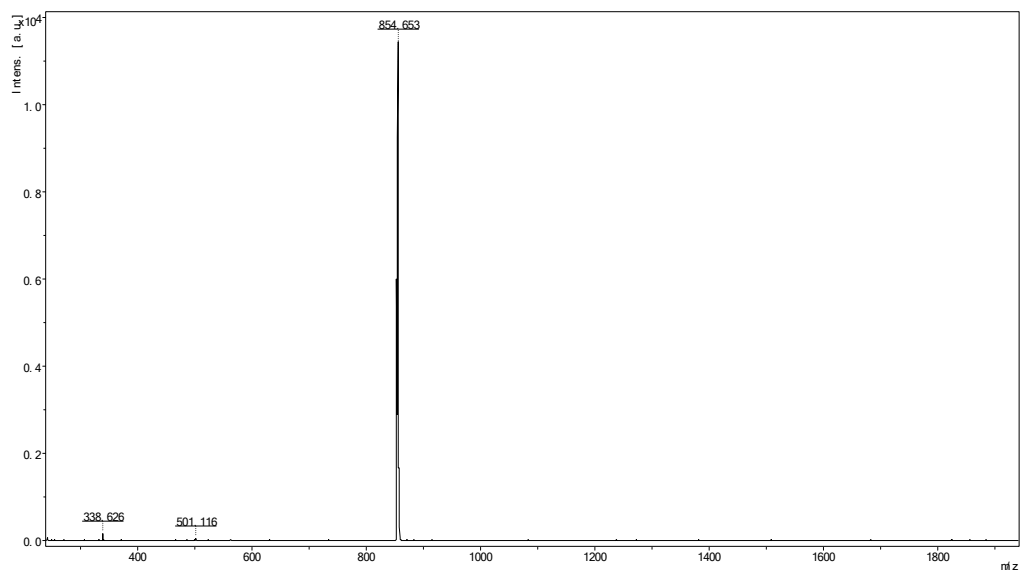


Fig S2 The  $^{13}\text{C}$ -NMR spectrum of **Ir1**.



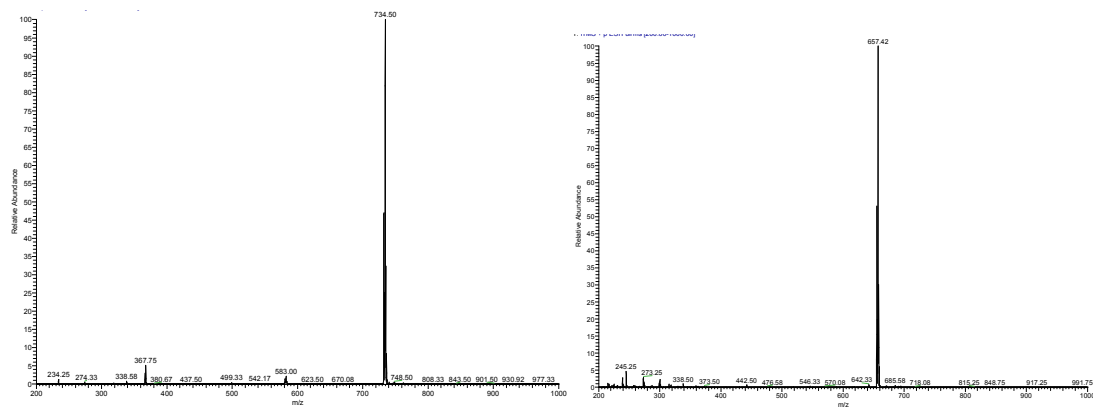


Fig S3 The MALDI-TOF-MS spectra of Ir1~Ir3.

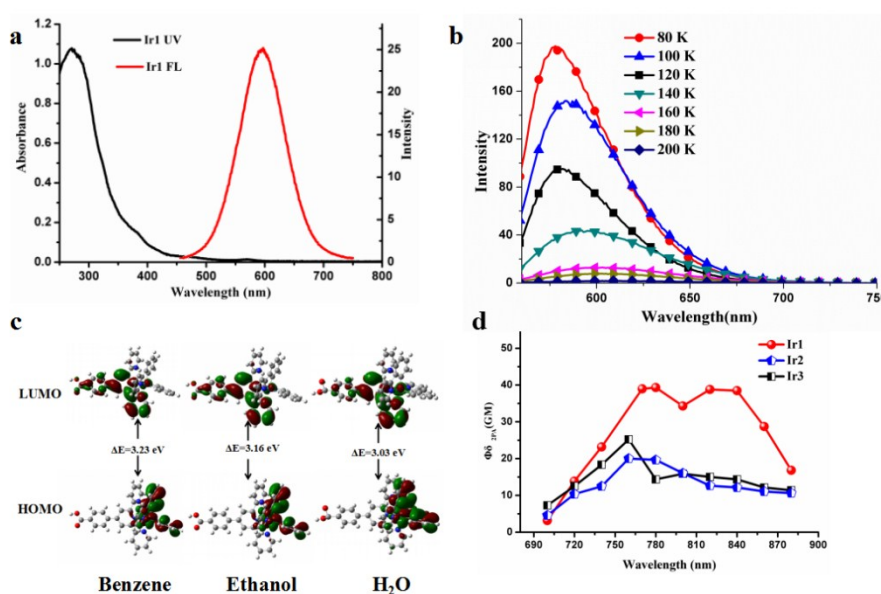


Fig S4(a) UV-vis absorption and one-photon fluorescence emission (OPEF) spectra of Ir1 in PBS buffer ( $c=10\mu\text{M}$ ) (b) OPEF spectra of Ir1 (MeTHF) from 80-200K. (c) Representation of calculated HOMO and LUMO orbitals of Ir1.(d) Two-photon absorption cross sections of Ir(III) complexes in DMSO/water (DMSO:H<sub>2</sub>O = 1:9) with excited wavelength from 700 nm to 900 nm.

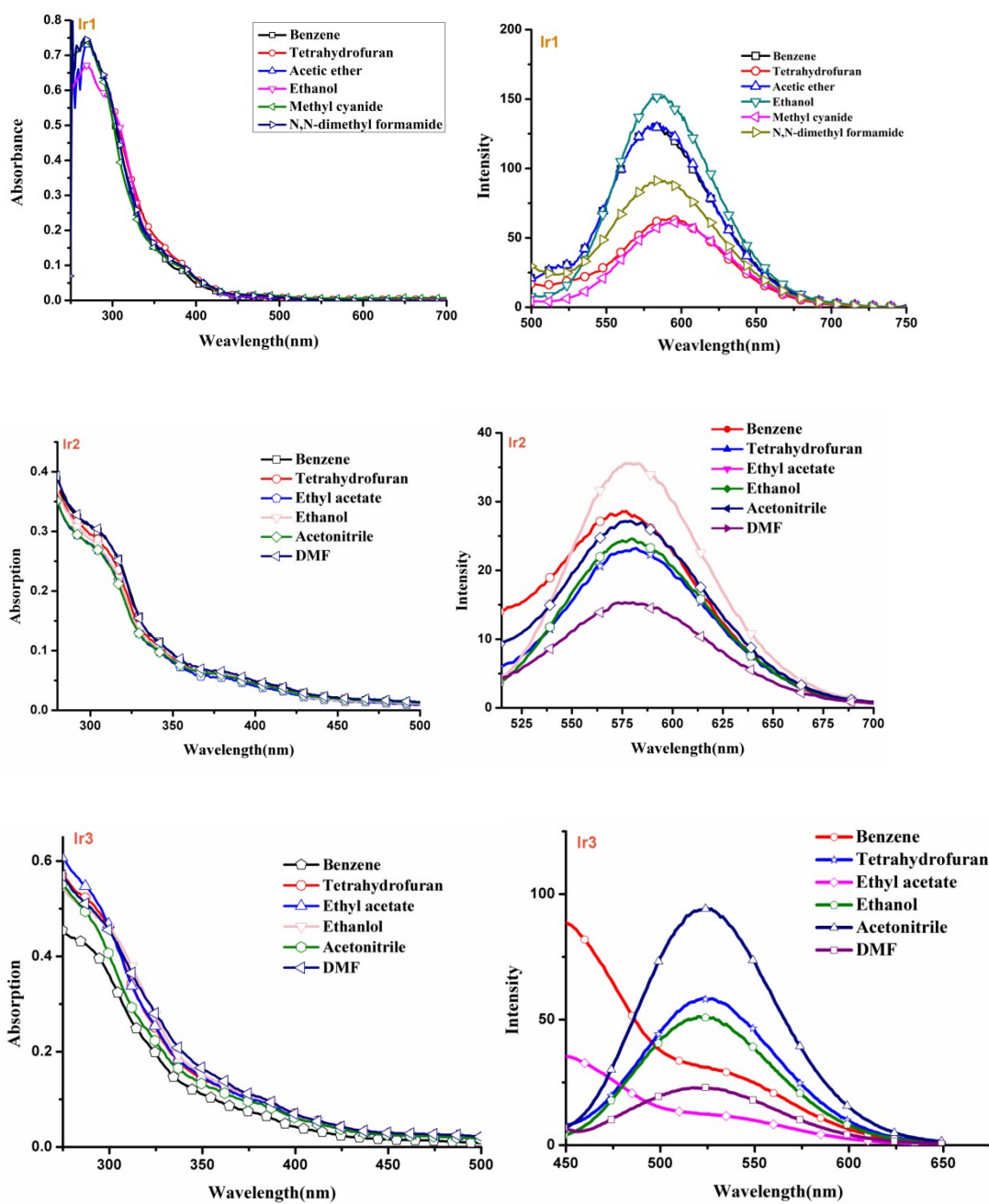


Fig S5 Linear absorption and linear emission spectra of **Ir1** in six organic solvents with a concentration of 10  $\mu\text{M}$ .

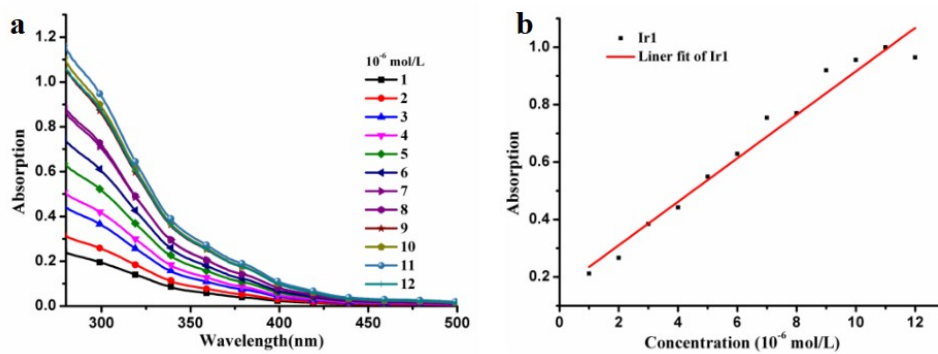


Fig S6 Absorption spectra (a) and plot of intensity against the concentration (b) of Ir1 in PBS buffer (PH = 7.4).

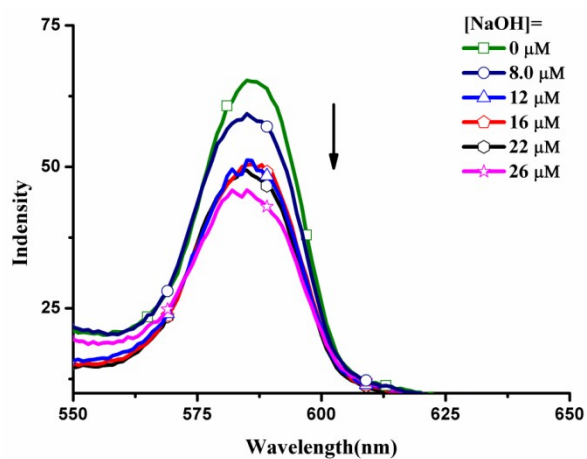


Fig. S7 OPEF spectra of Ir1([Ir1]=10  $\mu$ M) obtained in different NaOH concentrations.

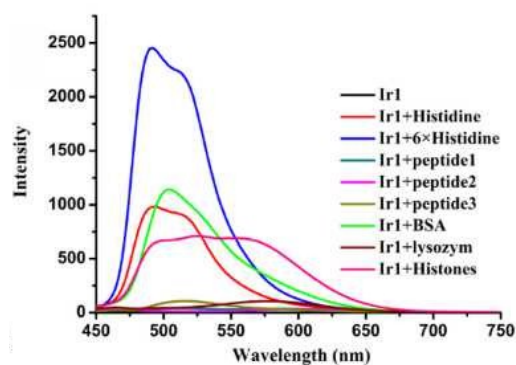


Fig. S8. Luminescence emission spectra of Ir1 (20 μM) in PBS buffer upon addition of 20 equiv histidine, 6×His, Arg-Trp-Ser-Asp-Thr-Tyr (peptide 1), Pro-Cys-Asn-Glu-Met-Leu (peptide 2), Val-Gly-Ala-Lys-Gln-Phe (peptide 3), lysozyme, BSA or histones which has different number of histidine residues.

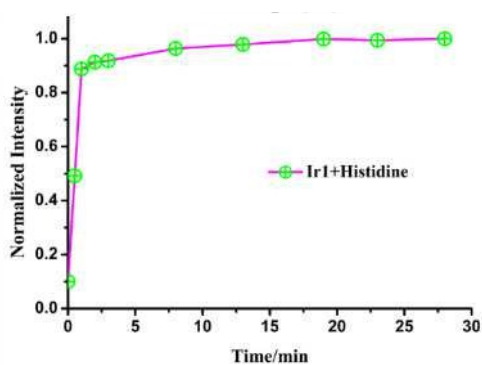


Fig. S9. Time-dependent emission intensity of Ir1 (20 μM) in the presence of histidine (10 equiv) in PBS buffer.

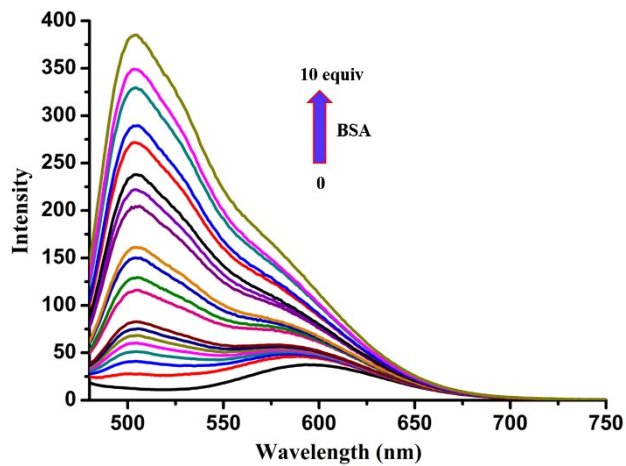


Fig S10 Changes in the luminescence emission spectra of **Ir1** (20 μM) with various amounts of BSA (0-10 equiv) in PBS buffer.

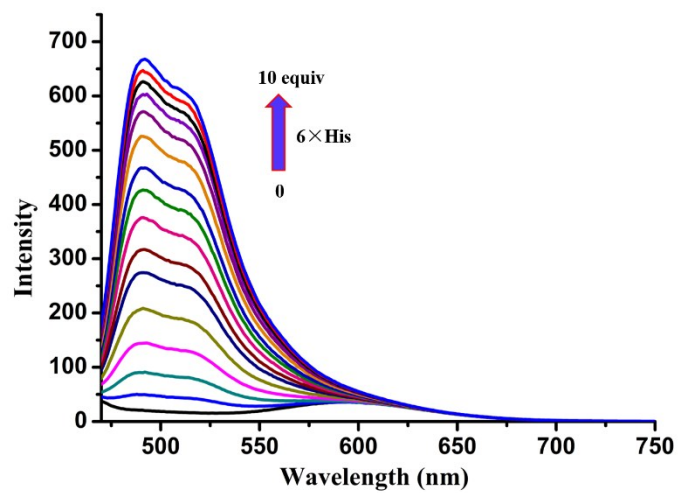


Fig. S11 Changes in the luminescence emission spectra of **Ir1** (20 μM) with various amounts of 6×His (0-10 equiv) in PBS buffer.

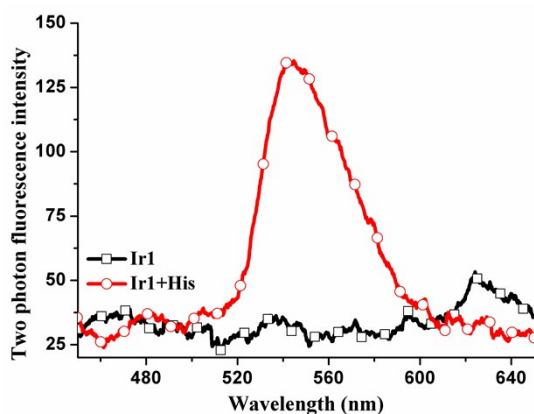


Fig. S12 Two-photon fluorescence spectra of **Ir1** in the presence or absence of His in PBS buffer

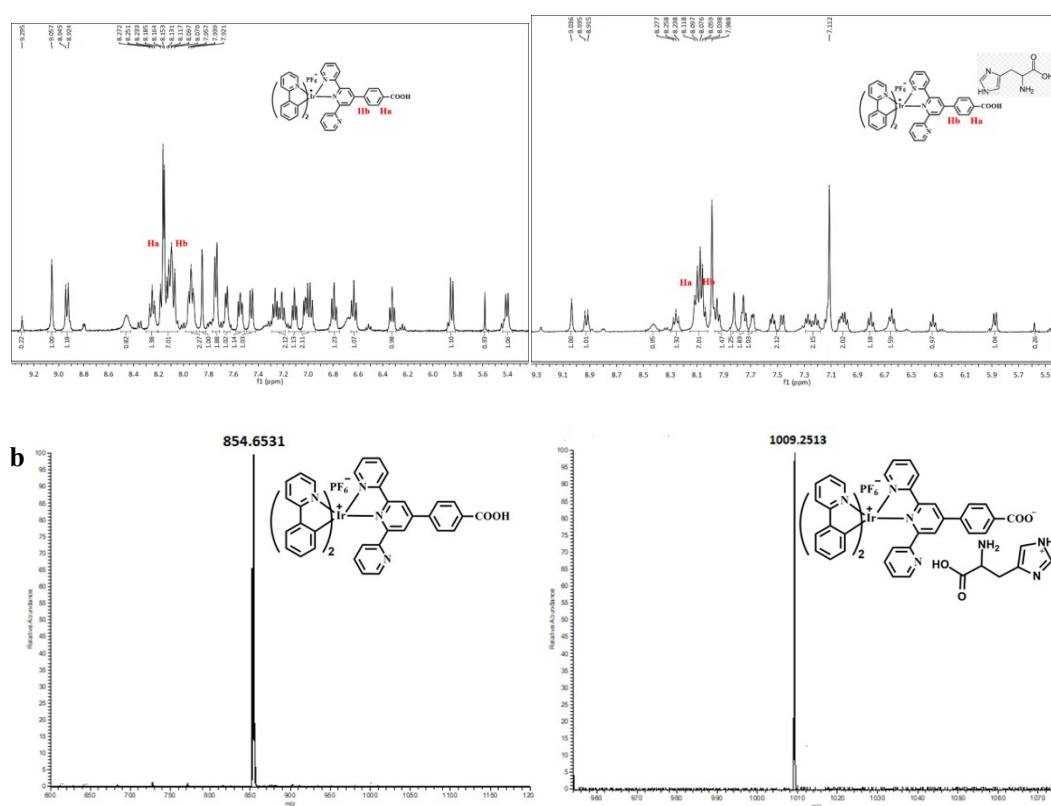


Fig. S13 (a)  $^1\text{H}$  NMR spectra change and of **Ir1** in the absence and presence of 10 equiv histidine in  $d_6$ -DMSO :  $\text{D}_2\text{O}$ =9:1 (v/v). (b) HRMS of **Ir1** in the absence and presence of histidine in PBS solution.

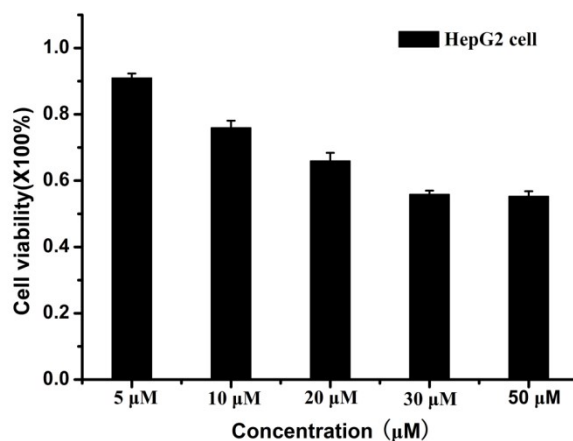


Fig S14 Cytotoxicity data results of **Ir1** obtained from the MTT assay.

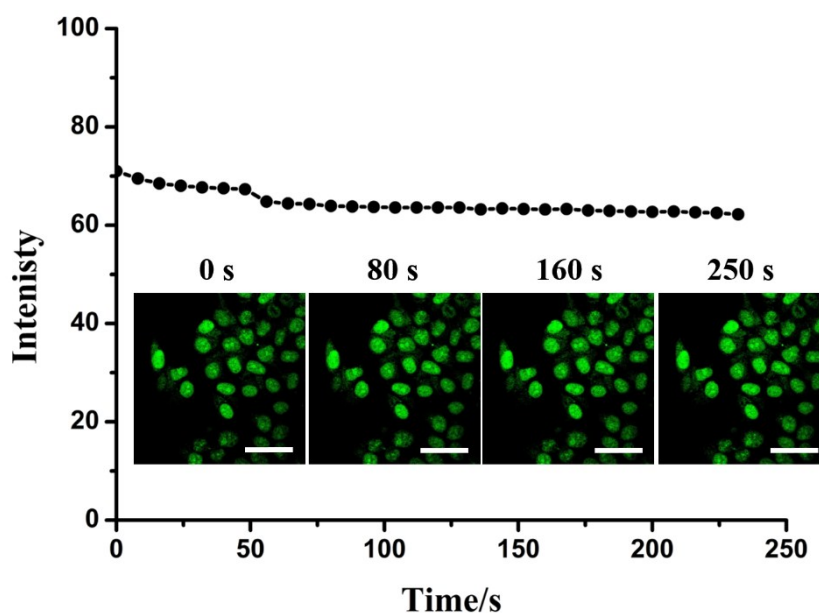


Fig S15 The photobleaching property of **Ir1**

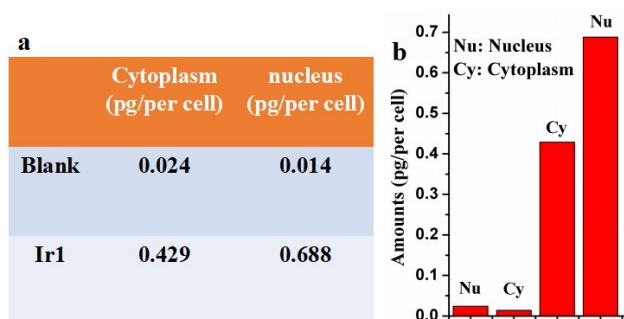


Fig S16 (a-b) Subcellular distribution of iridium in HepG2 cell incubation with **Ir1**. The amount

of iridium in cytoplasm and nucleus fractions was measured by ICP-MS. Data were collected at least three times independently.

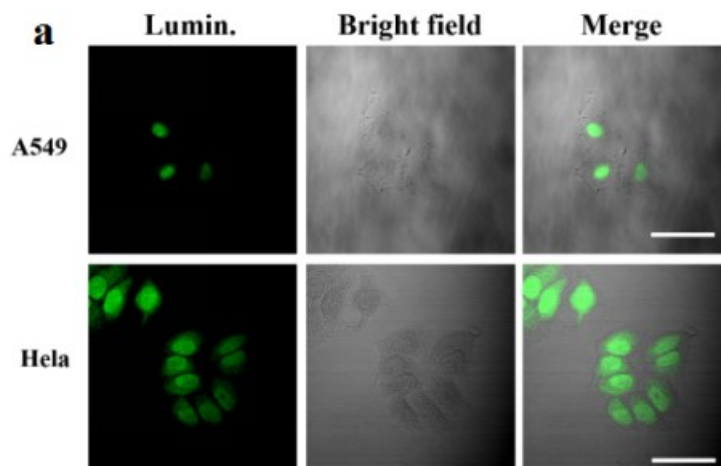


Fig S17 Confocal two-photon fluorescence images of living A549, HeLa cells incubated with 10  $\mu\text{M}$  **Ir1** in DMSO/PBS (pH = 7.4, 1:99 v/v) for 10 min at 37 °C ( $\lambda_{\text{ex}}$  = 820 nm,  $\lambda_{\text{em}}$  = 580-620 nm, scale bar = 20 $\mu\text{m}$ ).

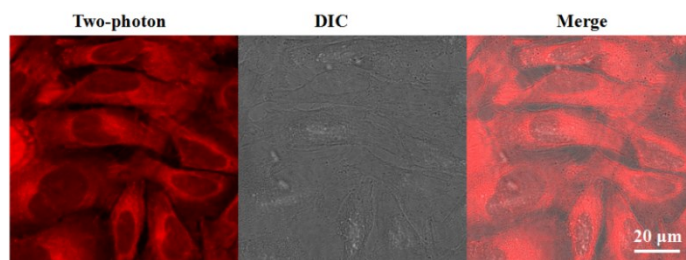


Fig S18 Two-photon micrographs for living HELF cells treated with **Ir1** and merged with DIC channel.

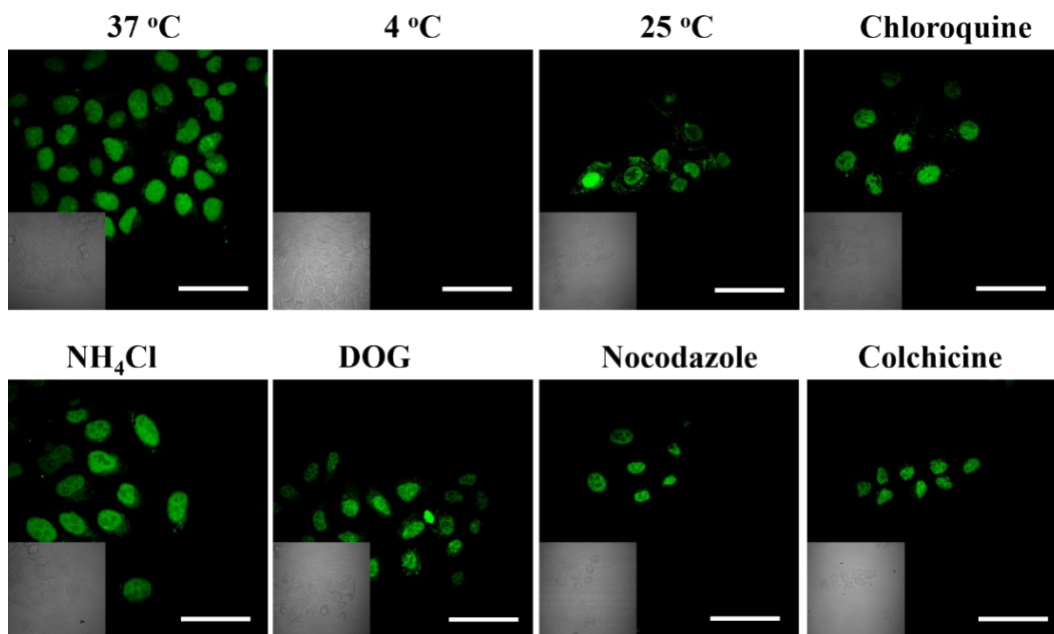


Fig S19 Mechanism of cellular uptake of **Ir1** (scale bar = 20 $\mu$ m)

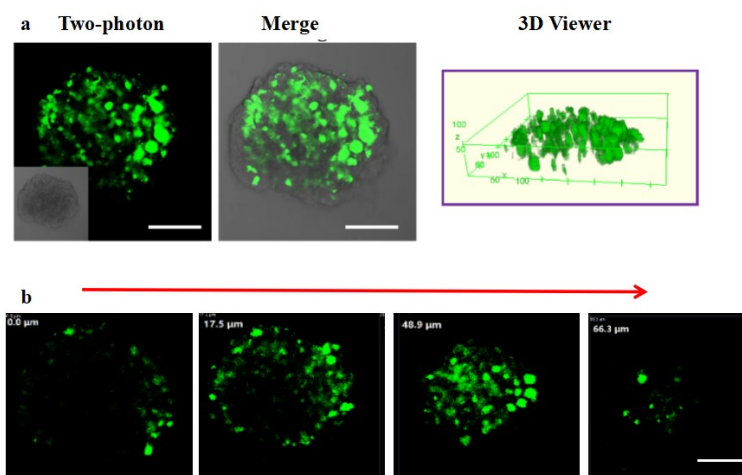


Fig S20 Two-photon fluorescence images of the 3D multicellular spheroids of HepG2 cells treated with 10  $\mu$ M **Ir1** for 5 h. (scale bar = 5  $\mu$ m)

Table S1 The photophysical data of the complex **Ir1** and **Ir1-His** in different solvents

<b>Ir1</b>	Solvents	$\lambda_{\max}^{abs}$ (nm) <sup>[a]</sup>	$\epsilon_{\max}^b$	$\lambda_{\max}^{SPEF}$ (nm) <sup>[c]</sup>	$\tau^{[d]}$	$\Delta\nu$ (nm) <sup>[e]</sup>	$\Phi^{[f]}$
	Benzene	383	1.06	583	33.22	200	0.37
	Tetrahydrofuran	382	0.97	592	27.35	210	0.20
	Ethyl acetate	384	0.97	581	29.24	197	0.38
	Ethanol	383	0.93	588	44.32	205	0.41
	Acetonitrile	383	0.93	595	37.28	212	0.17
	DMF	383	0.98	585	37.47	202	0.29
	PBS	375	1.08	595	37.55	201	0.09
<b>Ir1-His</b>	PBS	382	1.18	493	97.88	111	0.48

<sup>a</sup> Absorption peak position in nm ( $1 \times 10^{-5}$  mol L<sup>-1</sup>). <sup>b</sup> Maximum molar absorbance in  $10^5$  mol<sup>-1</sup> L cm<sup>-1</sup>. <sup>c</sup> Peak position of SPEF in nm ( $1.0 \times 10^{-5}$  mol L<sup>-1</sup>), excited at the absorption maximum. <sup>d</sup> fluorescence lifetime (ns) <sup>e</sup> Stokes shift in cm<sup>-1</sup>. TPEF peak position in nm pumped by femtosecond laser pulses at 300 mw at their maximum excitation wavelength. <sup>f</sup> Quantun yields determined by using coumarin 307 ( $\phi = 0.56$ ) ( $1.0 \times 10^{-5}$  mol L<sup>-1</sup>) as the standard.

Table S2 Calculated triplet transitions and the frontier orbitals of **Ir1**

state	energy/eV (nm)	molecular orbital	main transition character
T1	2.31 (567.9)	181 (H) → 182 (L)	<sup>3</sup> MLCT
T2	2.59 (477.9)	181 (H) → 185 (L+3)	<sup>3</sup> LLCT+ <sup>3</sup> MLCT

T3	2.83 (331.9)	179 (H-2) → 185 (L+3)	<sup>3</sup> LC
----	--------------	-----------------------	-----------------

Table S3 Calculated triplet transitions and the frontier orbitals of **Ir1**-histidine.

energy/eV (nm)	Oscillator	molecular orbital	main transition character
2.48 (498.5)	0.0043	222 (H) → 224 (L+1) (0.70)	$\pi \rightarrow \pi^*$ LLCT

Table S4 Crystal data and structure refinement for Ir2.

Identification code	1585448
Empirical formula	C <sub>35</sub> H <sub>27</sub> F <sub>1.5</sub> IrN <sub>7</sub> P <sub>0.25</sub>
Formula weight	774.08
Temperature/K	293
Crystal system	monoclinic
Space group	C2/m
a/Å	18.259(4)
b/Å	24.563(6)
c/Å	17.810(4)
$\alpha$ /°	90
$\beta$ /°	104.946(3)
$\gamma$ /°	90
Volume/Å <sup>3</sup>	7717(3)
Z	8

$\rho_{\text{calc}}/\text{cm}^3$	1.332
$\mu/\text{mm}^{-1}$	3.508
F(000)	3042.0
Radiation	MoK $\alpha$ ( $\lambda = 0.71073$ )
2 $\Theta$ range for data collection/ $^\circ$	2.366 to 52
Index ranges	$-22 \leq h \leq 22, -30 \leq k \leq 29, -21 \leq l \leq 21$
Reflections collected	29771
Independent reflections	7756 [ $R_{\text{int}} = 0.0624, R_{\text{sigma}} = 0.0607$ ]
Data/restraints/parameters	7756/666/397
Goodness-of-fit on $F^2$	1.075
Final R indexes [ $I \geq 2\sigma(I)$ ]	$R_1 = 0.0587, wR_2 = 0.1646$
Final R indexes [all data]	$R_1 = 0.0854, wR_2 = 0.1794$
Largest diff. peak/hole / $e \text{ \AA}^{-3}$	3.71/-1.65

1. Demas, J. N. and Crosby, G. A. Measurement of photoluminescence quantum yields. Review. *J. Phys. Chem.*, 1971, 75, 991-1024.

2. Gray, T. G.; Rudzinski, C. M.; Meyer, E. E.; Holm, R. H and Nocera, D. G. Spectroscopic and Photophysical Properties of Hexanuclear Rhenium(III) Chalcogenide Clusters. *J. Am. Chem. Soc.*, 2003, 125, 4755-4770.

3. Wang, H.; Hu L.; Du, W.; Tian, X. H.; Hu, Z. J.; Zhang, Q.; Zhou, H. P.; Wu, J. Y.; Uvdal, K.

And Tian, Y. P. , Mitochondria-targeted Iridium (III) complex as two-photon fluorogenic probes of cysteine/homocysteine. *Sensors and Actuators B*. **2018**, 255, 408-415

4. Venkatachalam, C. M.; Jiang, X.; Oldfield, T.; Waldman, M. LigandFit: a novel method for the shape-directed rapid docking of ligands to protein active sites. *J. Mol. Graph. Model* 2003, 21, 289-307.